Data Collection	KiDS
Release Number	3.1
Data Provider	Konrad Kuijken
Date	27.12.2016

ESO Science Archive Facility - Phase 3 Data Release Description
ESO public survey programme KIDS - The Kilo-Degree Survey (VST), Data Release DR3.1
provided by K. Kuijken, submitted between 2016-12-09 and 2016-12-20, published on 2017-01-03

Abstract

This catalogue data release contains the weak lensing shear measurements from the KiDS-450 data set, which corresponds to the survey area of the third public release of the Kilo-Degree Survey (KiDS). KiDS is an ESO public survey carried out with the VLT Survey Telescope and Omega-CAM camera, that will image 1500 square degrees in four filters (*u, g, r, i*), in single epochs per filter. KiDS is designed to be a weak lensing shear tomography survey, and has as its core science drivers mapping of the large-scale matter distribution in the universe and constraining the equation-of-state of Dark Energy. The catalogue released here constitutes the first weak lensing shear data set from KiDS with which these questions have been addressed (Hildebrandt & Viola et al. 2017, MNRAS, 465, 1454).

The data were taken under ESO programme IDs: 177.A-3016(A), 177.A-3016(B), 177.A-3016(C), 177.A-3016(D), 177.A-3016(E), 177.A-3016(G), 177.A-3016(J), 177.A-3016(K), 177.A-3017(A), and 177.A-3018(A).

Overview of Observations

The DR3.1 shear catalogue is based on observations of 454 KiDS survey tiles in all four filters (*u,g,r,i*). Figure 1 shows the locations of the included tiles within the survey fields.

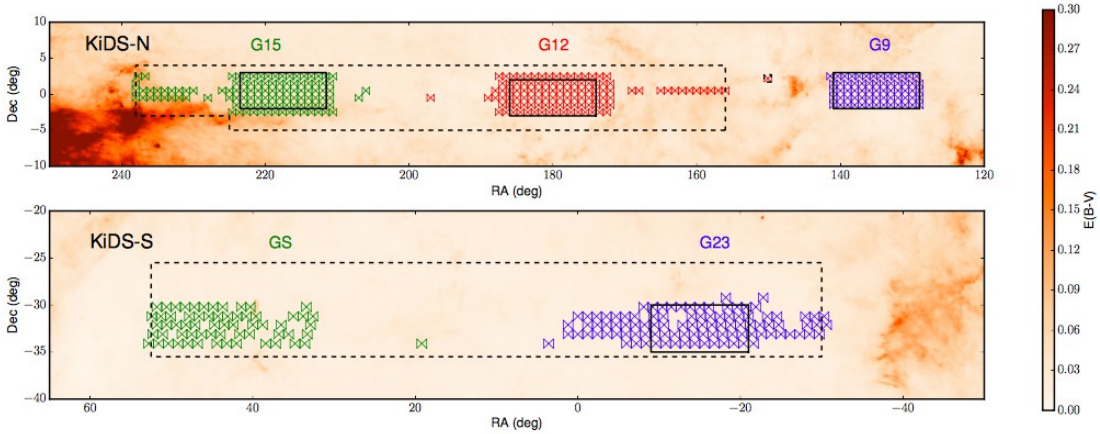

Fig. 1: Sky distribution of tiles included in the catalogue. The dashed and solid lines outline the full KiDS survey area and the areas observed by the GAMA spectroscopic survey, respectively. Coloured symbols correspond to included pointings, with the colours representing five patches (G9, G12, G15, G23, GS). The background shows E(B-V) reddening maps from Schlegel et al. (1998, ApJ. 500, 525).

Release Content

Based on the 454 KiDS tiles indicated in Fig. 1, the total area covered by the shear catalog is 449.7 sq.deg. after trimming of the edges of individual tiles. Masking of bright stars, satellite trails and other image defects results in an effective area of 360.3 sq.deg. Source detection was done on

stacked *r*-band images, after which galaxy shapes were measured on individual sub-exposures. The included photometry and photometric redshifts are based on 4-band *ugri* image stacks.

Only galaxies with reliable shape measurements are included in this catalogue. Unreliable sources have been rejected based on several criteria listed in Hildebrandt & Viola et al. (2017, MNRAS, 465, 1454). The faint limit of the catalogue is $r = 25.0$, corresponding to a typical signal-to-noise of 5 σ. The catalogue contains a total of 14,650,348 sources, is made up of 455 files (454 data files and 1 metadata file), and has a total data volume of 4.14 GB

Release Notes

Data processing for this release was performed by the KiDS collaboration and is extensively described in a number of publications. Below is a very brief description with references and links to the more detailed sources.

Data Reduction and Calibration

Two data reduction pipelines were used for the production of this data release.
The *r*-band data of the included tiles was reduced with the THELI pipeline (Erben et al. 2013, MNRAS, 433, 2545) and source detection was done on the resulting stacks. Shapes of objects were measured with *lens*fit (Miller et al. 2013, MNRAS, 429, 2858; Fenech Conti et al. 2016) on the single *r-band* exposures to avoid any systematics introduced by resampling or stacking.
The photometry included in the catalogue was measured from *ugri* stacks produced with Astro-WISE (McFarland et al. 2013, ExA, 35, 45), following the same procedures as used for KiDS DR3. Photometric redshifts were derived using the Bayesian template fitting method BPZ (Benítez, 2000, ApJ, 536, 571). The following documents and publications provide detailed information regarding the various data processing steps.

KiDS *r*-band THELI processing and photometric methods and redshifts:

- Kuijken et al. 2015, MNRAS, 454, 3500

*Lens*fit shape measurements:

- Hildebrandt & Viola et al., 2017, MNRAS, 465, 1454
- Fenech Conti et al. 2016, MNRAS, submitted, arXiv:1606.05337

KiDS *ugri* processing and photometric calibration:

- De Jong et al. 2017, in prep.
- KiDS DR3 website and release notes

Data Quality

The quality and reliability of the KiDS data and the derived photometry, redshifts and shape measurements are reviewed in great detail in the following publications:

KiDS photometric redshifts and *r*-band image quality:

- Kuijken et al. 2015, MNRAS, 454, 3500

*Lens*fit shape measurements:

- Hildebrandt & Viola et al., 2017, MNRAS, 465, 1454

KiDS ugri data and photometry:

- de Jong et al. 2015, A&A, 582, A62
- De Jong et al. 2017, in prep.

Known issues

Please note that the source IDs in this catalogue may differ slightly from the ones included in the KiDS DR3.0 release.

c-terms

In the KiDS-450 cosmic shear analysis Hildebrandt & Viola et al. (2017) found small residual c-terms (non-zero average shear). These were subtracted patch by patch, and tomographic bin by tomographic bin, before computing the shear-shear correlation functions. Any science analysis for which c terms are deemed important should determine these from the data. Note that the *lens*-fit weights should be used to compute the averages.

Previous Releases

This catalogue release constitutes the first official release of weak lensing shear data by KiDS and corresponds almost exactly with the area for which other data products were released in the preceding general KiDS data releases (DR1, DR2 and DR3).

Scientific publications

Use of these data in rigorous scientific analyses is the ultimate test of the data quality. The following scientific analyses were performed using this shear catalogue prior to release:

- Hildebrandt & Viola et al., 2017, MNRAS, 465, 1454
- Fenech Conti et al. 2016, MNRAS, submitted, arXiv:1606.05337
- Joudaki et al. 2016, MNRAS, submitted, arXiv:1610.04606

Data Format

Files Types

Because of size restrictions the catalogue is submitted in multiple files, and consists of a metadata file and a catalogue data file for each tile. The data files have the central coordinates of the corresponding tile encoded in the filename, following the convention:

`KiDS_DR3.1_131.0_-0.5_ugri_shear.fits`

The metadata file, which contains only metadata and no catalogue data, is called:

`KiDS_DR3.1_ugri_shear.fits`

Catalogue Columns

The table below lists the columns that are present in the KiDS DR3.1 shear catalogue. It is divided in a number of subsections grouping columns resulting from a common data product or software package.

In the following, we provide additional information on a number of columns.

i. `KIDS_TILE`: name of the KiDS survey tile in which the source is located. Searching the ESO archive with this `OBJECT` name will link to further data products for this tile.
ii. `THELI_NAME`: name for the survey tile in the THELI pipeline; for scripting reasons the '.' and '-' characters are replaced with 'p' and 'm', respectively.
iii. `MASK`: bit mask indicating sources affected by different types of defects. Automatic and manual masks produced during data processing flag areas affected by bright stars (e.g. saturated pixels, reflection halos, diffraction and readout spikes) and other severe image defects. In the released catalogue the most strongly affected regions are already removed,

leaving only sources with reliable measurements. As a result, only the following bit mask values are present:

Mask bit value	Type of area
2	Faint stellar reflection halo
64	u-band AstroWISE manual mask
128	g-band AstroWISE manual mask
256	r-band AstroWISE manual mask
512	i-band AstroWISE manual mask

iv. `Flag`: SExtractor extraction flag. Many sources that are flagged during source detection are removed from the catalogue based on the *lens*fit results because they do not provide reliable shape measurements. The flag values that are still present in the catalogue are:

Flag value	Type
1	The object has neighbours, bright and close enough to significantly bias the photometry, or bad pixels (more than 10% of the integrated area affected)
2	The object was originally blended with another one
16	Obejcts's aperture data are incomplete or corrupted

v. `SG_FLAG`: star-galaxy separator based on analysis of the second and fourth order image moments of the source; 0 = star, 1 = galaxy

vi. `MAG_u/g/r/i`: the magnitudes are based on Gaussian Aperture and Photometry (GAaP) measurements and are dereddened and colour-calibrated using stellar locus regression. Note: these aperture magnitudes are mainly intended for colour measurements, since they only probe the central regions of the source. They are not total magnitudes, except in the case of unresolved or point sources.

vii. `MAG_LIM_u/g/r/i`: local limiting magnitude, defined as the magnitude corresponding to a flux equal to the 1σ flux error.

viii. `ZPT_offset`: the magnitudes reported in this catalogue have been colour-calibrated, but their absolute calibration has only been homogenized per survey tile, not over the full area. Based on a comparison (see de Jong et al. 2016, in prep) of the *r*-band magnitudes with the GAIA DR1 (GAIA Collaboration, 2016, arXiv:1609.04172) we provide these additional photometric offsets that can be used to homogenize the photometry over the whole catalogue. The reported offsets are with respect to the GAIA photometry, but can be used to calibrate the photometry to the SDSS photometric system as follows:

`mag_u/g/r/i_homogenized = mag_u/g/r/i – ZPT_offset + 0.049`

Note: if used, these offsets must be applied to the magnitudes in *all* filters!

ix. `T_B`: the best-fit spectral template for each source; these values correspond to the following types, where fractional types can occur because the templates are interpolated: 1=CWW-Ell, 2=CWW-Sbc, 3=CWW-Scd, 4=CWW-Im, 5=KIN-SB3, 6=KIN-SB2 (Capak, 2004, PhD. thesis, Univ. Hawai'i).

x. `ODDS`: a measure of the uni-modality of the redshift Probability Distribution Function; a higher value indicates a higher reliability of the best photo-z estimate.

xi. `fitclass`: *lens*fit object class; the only classes included in the catalogue are 0 (galaxy, no issues) and -9 (large galaxy, overfills 48 pixel postage stamp size). The latter class is retained to avoid ellipticity selection bias in the brightest galaxy sample.

xii. `n_exposures_used`: the number of *r*-band sub-exposures for which *lens*fit measured the shape of the source. Due to the dither pattern, or near tile edges, some sources are only present in a subset of the 5 sub-exposures.

xiii. `e1` or `e2`: *lens*fit shear estimators. Note: the `e2` component is defined relative to the RAJ2000, DECJ2000 grid; depending on the user's definition of angles in this reference frame, the sign of `e2` may need to be changed.

xiv. `PSF_e1` and `PSF_e1_exp[k]`: model PSF ellipticities at the location of the object, in this case the real part of ε_{PSF}. `PSF_e1_exp[k]` is the PSF ellipticity in sub-exposure number k, while `PSF_e1` refers to the average over all exposures used.

xv. `m`: the multiplicative shear calibration correction which should be applied in an ensemble average, rather than on a galaxy-by-galaxy basis (see Fenech Conti et al 2016 arXiv:1606.05337). Averaged catalogued ellipticities should be divided by 1+<m>, where the ellipticities should be weighted with the *lens*fit `weight`.

Label	Format	Unit	Description
General source parameters			
ID	25A		Source identifier
RAJ2000	1D	deg	Right ascension of barycenter (J2000)
DECJ2000	1D	deg	Declination of barycenter (J2000)
Patch	3A		Patch (G9, G12, G15, G23 or GS)
SeqNr	1J		Running object number within the patch
KIDS_TILE	16A		Name of survey tile
THELI_NAME	16A		THELI name for the tile
MASK	1J		Mask value at the object position
SG_FLAG	1E		Star-galaxy separator (0=star, 1=galaxy)
r-band SExtractor output			
KRON_RADIUS	1E	pixel	Scaling radius of the ellipse for magnitude measurements
Xpos	1E	pixel	Object position along x in the r-band THELI stack (non unique)
Ypos	1E	pixel	Object position along y in the r-band THELI stack (non unique)
FWHM_IMAGE	1E	pixel	r-band FWHM assuming a Gaussian core
FWHM_WORLD	1E	deg	r-band FWHM assuming a Gaussian core
Flag	1J		r-band SExtractor extraction flags
FLUX_RADIUS	1E	pixel	r-band half-light radius
CLASS_STAR	1E		r-band SExtractor S/G classifier output
Photometry measurements			
MAG_u	1E	mag	Magnitude in the u-band (GAaP, dereddened)
MAGERR_u	1E	mag	Magnitude error in the u-band
MAG_g	1E	mag	Magnitude in the g-band (GAaP, dereddened)
MAGERR_g	1E	mag	Magnitude error in the g-band
MAG_r	1E	mag	Magnitude in the r-band (GAaP, dereddened)
MAGERR_g	1E	mag	Magnitude error in the r-band
MAG_i	1E	mag	Magnitude in the i-band (GAaP, dereddened)
MAGERR_i	1E	mag	Magnitude error in the i-band
MAG_LIM_u	1E	mag	Local 1σ limiting magnitude in the u-band
MAG_LIM_g	1E	mag	Local 1σ limiting magnitude in the g-band
MAG_LIM_r	1E	mag	Local 1σ limiting magnitude in the r-band
MAG_LIM_i	1E	mag	Local 1σ limiting magnitude in the i-band
ZPT_offset	1E	mag	Zeropoint offset derived from GAIA DR1 G photometry

Label	Format	Unit	Description
BPZ output			
Z_B	1E		BPZ best redshift estimate; peak of posterior probability distribution
Z_B_MIN	1E		Lower bound of the 95% confidence interval of Z_B
Z_B_MAX	1E		Upper bound of the 95% confidence interval of Z_B
T_B	1E		Spectral type corresponding to Z_B
ODDS	1E		Empirical ODDS of Z_B
***lens*fit output**			
fitclass	1I		Lensfit fit class
bias_corrected_scalelength	1E		Lensfit galaxy model scalelength
bulge_fraction	1E		Lensfit galaxy model bulge-fraction B/T
model_flux	1E	counts	Lensfit galaxy model flux
pixel_SNratio	1E		Lensfit data S/N ratio
model_SNratio	1E		Lensfit model S/N ratio
contamination_radius	1E	pixel	Distance to nearest contaminating isophote
PSF_e1	1E		Lensfit PSF model mean ellipticity e1
PSF_e2	1E		Lensfit PSF model mean ellipticity e2
PSF_Strehl_ratio	1E		Lensfit PSF model mean pseudo-Strehl ratio
PSF_Q11	1E		2nd order brightness moment Q11 of the PSF
PSF_Q22	1E		2nd order brightness moment Q22 of the PSF
PSF_Q12	1E		2nd order brightness moment Q12 of the PSF
n_exposures_used	1E		Number of r-band exposures used in lensfit measurements
PSF_e1_exp1	1E		Lensfit PSF model ellipticity e1 of exposure 1
PSF_e2_exp1	1E		Lensfit PSF model ellipticity e2 of exposure 1
PSF_e1_exp2	1E		Lensfit PSF model ellipticity e1 of exposure 2
PSF_e2_exp2	1E		Lensfit PSF model ellipticity e2 of exposure 2
PSF_e1_exp3	1E		Lensfit PSF model ellipticity e1 of exposure 3
PSF_e2_exp3	1E		Lensfit PSF model ellipticity e2 of exposure 3
PSF_e1_exp4	1E		Lensfit PSF model ellipticity e1 of exposure 4
PSF_e2_exp4	1E		Lensfit PSF model ellipticity e2 of exposure 4
PSF_e1_exp5	1E		Lensfit PSF model ellipticity e1 of exposure 5
PSF_e2_exp5	1E		Lensfit PSF model ellipticity e2 of exposure 5
e1	1E		Lensfit galaxy e1 expectation value
e2	1E		Lensfit galaxy e2 expectation value
weight	1E		Lensfit inverse variance shear weight
m	1E		Multiplicative shear calibration

Acknowledgements

Users of these data should include the following acknowledgment to the source of the data:

Based on data products from observations made with ESO Telescopes at the La Silla Paranal Observatory under programme IDs 177.A-3016, 177.A-3017 and 177.A-3018.

and should cite Hildebrandt & Viola et al. (2017), Fenech Conti et al. (2016) and accompanying papers as follows:

We use cosmic shear measurements from the Kilo-Degree Survey (Kuijken et al. 2015, Hildebrandt et al. 2017, Fenech Conti et al. 2016), hereafter referred to as KiDS. The KiDS data are processed by THELI (Erben et al. 2013) and Astro-WISE (McFarland et al. 2013, de Jong et al. 2015). Shears are measured using lensfit (Miller et al. 2013), and photometric redshifts are obtained from PSF-matched photometry and calibrated using external overlapping spectroscopic surveys (see Hildebrandt & Viola et al. 2017).